

International Journal of Modern Physics: Conference Series  
 © World Scientific Publishing Company

## SINGLE SPIN ASYMMETRY IN HIGH ENERGY QCD

YURI V. KOVCHegov \*

*Department of Physics, The Ohio State University  
 Columbus, OH 43210, USA  
 kovchegov.1@asc.ohio-state.edu*

MATTHEW D. SIEVERT

*Department of Physics, The Ohio State University  
 Columbus, OH 43210, USA  
 sievert.7@osu.edu*

We present the first steps in an effort to incorporate the physics of transverse spin asymmetries into the saturation formalism of high energy QCD. We consider a simple model in which a transversely polarized quark scatters on a proton or nuclear target. Using the light-cone perturbation theory the hadron production cross section can be written as a convolution of the light-cone wave function squared and the interaction with the target. To generate the single transverse spin asymmetry (STSA) either the wave function squared or the interaction with the target has to be  $T$ -odd. In this work we use the lowest-order  $q \rightarrow qG$  wave function squared, which is  $T$ -even, generating the STSA from the  $T$ -odd interaction with the target mediated by an odderon exchange. We study the properties of the obtained STSA, some of which are in qualitative agreement with experiment: STSA increases with increasing projectile  $x_F$  and is a non-monotonic function of the transverse momentum  $k_T$ . Our mechanism predicts that the quark STSA in polarized proton–nucleus collisions should be much smaller than in polarized proton–proton collisions. We also observe that the STSA for prompt photons due to our mechanism is zero within the accuracy of the approximation.

*Keywords:* single transverse spin asymmetry; parton saturation; odderon.

PACS numbers: 24.85.+p, 12.38.Bx, 13.88.+e, 24.70.+s

### 1. Introduction

This presentation is based on the paper [1].

Our goal is to use the saturation/Color Glass Condensate (CGC) formalism (see [2, 3, 4] for reviews) to calculate the single transverse spin asymmetry (STSA) in polarized proton–proton and polarized proton–nucleus collisions. The observable is

\*Presented by YK at the *QCD Evolution Workshop*, May 14 - 17, 2012, Thomas Jefferson National Accelerator Facility, Newport News, VA.

2 Yuri V. Kovchegov, Matthew D. Sievert

defined by

$$A_N(\mathbf{k}) \equiv \frac{\frac{d\sigma^\uparrow}{d^2k dy} - \frac{d\sigma^\downarrow}{d^2k dy}}{\frac{d\sigma^\uparrow}{d^2k dy} + \frac{d\sigma^\downarrow}{d^2k dy}} = \frac{\frac{d\sigma^\uparrow}{d^2k dy}(\mathbf{k}) - \frac{d\sigma^\uparrow}{d^2k dy}(-\mathbf{k})}{\frac{d\sigma^\uparrow}{d^2k dy}(\mathbf{k}) + \frac{d\sigma^\uparrow}{d^2k dy}(-\mathbf{k})} \equiv \frac{d(\Delta\sigma)}{2 d\sigma_{unp}} \quad (1)$$

where the arrow indicates spin-up and spin-down outgoing hadron with the spin direction taken here to be along the  $\hat{x}$ -axis (with  $\hat{z}$  the collision axis).

For simplicity we will consider scattering of a transversely polarized quark on an unpolarized proton or nuclear target  $q^\uparrow + A \rightarrow q + X$ . The realistic case of the incoming transversely polarized proton can be recovered if one convolutes the cross section we obtain with the polarized proton wave function squared, or, perhaps equivalently, with the proton transversity distribution.

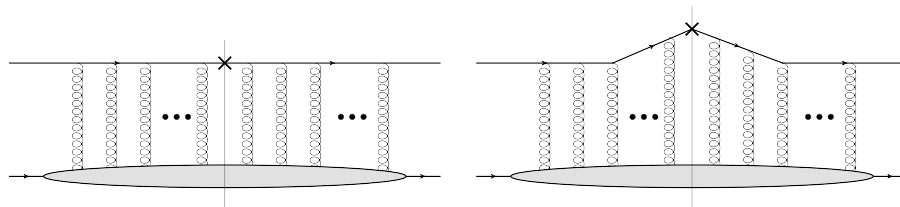


Fig. 1. Left panel: eikonal scattering of a quark on a nucleus. Right panel: quark–nucleus scattering with recoil.

Figure 1 demonstrates that to capture the spin-dependent effects, such as the STSA, one has to go beyond the eikonal accuracy in the calculation. Recoilless eikonal scattering, as shown in the left panel of Fig. 1, is spin-independent and can not generate the asymmetry. Naive inclusion of sub-eikonal corrections is possible by introducing recoil in the scattering, as shown in the right panel of Fig. 1: such diagrams are suppressed by a power of the center of mass energy squared  $s$  of the collision and are usually discarded in the saturation/CGC formalism since they are very small.

A much larger contribution to STSA may arise from the non-eikonal splitting of the projectile quark into a quark and a gluon,  $q \rightarrow qG$ , which is suppressed only by a power of the strong coupling  $\alpha_s$ . In the LCPT language the  $q \rightarrow qG$  splitting may take place either long before or long after the interaction with the target, as shown in Fig. 2 below. (Splitting during the interaction with the target is suppressed by powers of energy [5].) Both such contributions would be included in the light-cone wave function squared of the projectile (quark).

The spin-dependence by itself is insufficient to generate the STSA: one also needs a relative phase between the amplitude and the complex conjugate amplitude contributing to the STSA-generating part of the process [6, 7]. In the standard interpretation of the Sivers effect [8] both the spin-dependence and the relative phase originate in the wave function squared (though, often-times, the actual diagrammatic representation of the effect requires a final-state interaction with the

polarized projectile [7], which, in the CGC rapidity-ordered language, can still be incorporated as a final-state light-cone wave function [9]). The lowest-order  $q \rightarrow qG$  splitting from Fig. 2 is too basic to generate the phase. In the Collins mechanism the phase is generated in the fragmentation function [10]: this can certainly take place in the saturation/CGC framework as well, but is not the main aim of this investigation.

Below we show that it is also possible to generate the relative phase in the integration with the unpolarized target. We thus obtain a new mechanism for generating STSA, where the spin dependence comes from the polarized projectile wave function, while the phase arises in the interaction with the target.

## 2. Calculation of STSA in the Saturation Framework

The diagrams for the scattering process of a transversely polarized quark on a proton or nuclear target are shown in Fig. 2. Squaring the sum of these diagrams gives us the graphs shown in Fig. 3 which contribute to the inclusive quark production cross section.

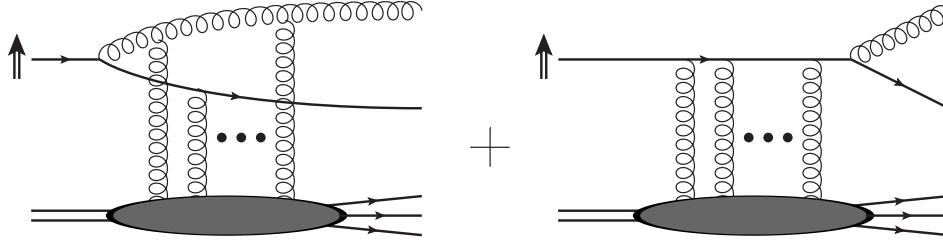


Fig. 2. Two contributions to the amplitude for the high energy quark–target scattering in LCPT.

The calculation proceeds along the standard steps employing the light-cone perturbation theory (LCPT) (see [4] for a review): the  $q \rightarrow qG$  splitting contributes to the light-cone wave function, which factorizes from the interaction with the target. The general result for the quark production in the  $q^\uparrow + A$  scattering given by diagrams in Fig. 3 reads

$$\frac{d\sigma^{(q)}}{d^2k dy_q} = \frac{C_F}{2(2\pi)^3} \frac{\alpha}{1-\alpha} \int d^2x d^2y d^2z e^{-ik \cdot (z-y)} \Phi_\chi(z-x, y-x, \alpha) \mathcal{I}^{(q)}(x, y, z) \quad (2)$$

with  $\Phi_\chi$  denoting the light-cone wave function squared and  $\mathcal{I}^{(q)}$  representing the interaction with the target with all the coordinate labels shown explicitly in Fig. 3. Here

$$\mathbf{u} = \mathbf{x} + \alpha(\mathbf{z} - \mathbf{x}) \quad (3a)$$

$$\mathbf{w} = \mathbf{x} + \alpha(\mathbf{y} - \mathbf{x}) \quad (3b)$$

4 Yuri V. Kovchegov, Matthew D. Sievert

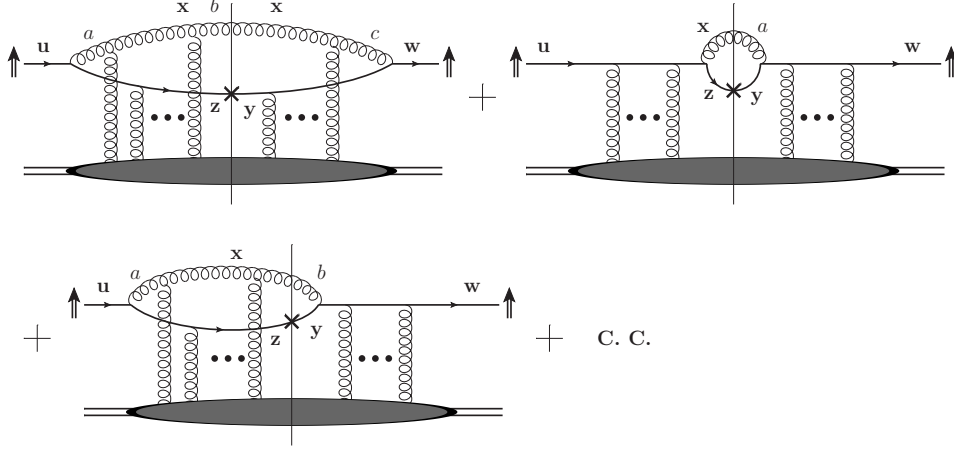


Fig. 3. The cross section for quark production in the polarized quark–nucleus scattering.

are the transverse coordinates of the incoming quark in the amplitude and in the complex conjugate amplitude, while  $\alpha$  is the fraction of the incoming quark's plus momentum component  $p^+$  carried by the produced quark with the plus momentum component  $k^+$ , such that  $\alpha = k^+/p^+$ .

The light-cone wave function squared  $\Phi_\chi$  can be decomposed into a polarization-independent term and another term which is proportional to the quark transverse polarization eigenvalue  $\chi$ ,

$$\Phi_\chi(z - \mathbf{x}, \mathbf{y} - \mathbf{x}, \alpha) = \Phi_{unp}(z - \mathbf{x}, \mathbf{y} - \mathbf{x}, \alpha) + \chi \Phi_{pol}(z - \mathbf{x}, \mathbf{y} - \mathbf{x}, \alpha), \quad (4)$$

where a straightforward calculation yields [1]

$$\begin{aligned} \Phi_{unp} = \frac{2\alpha_s}{\pi} \tilde{m}^2 \left[ (1 + \alpha^2) \frac{(z - \mathbf{x}) \cdot (\mathbf{y} - \mathbf{x})}{|z - \mathbf{x}| |\mathbf{y} - \mathbf{x}|} K_1(\tilde{m} |z - \mathbf{x}|) K_1(\tilde{m} |\mathbf{y} - \mathbf{x}|) \right. \\ \left. + (1 - \alpha)^2 K_0(\tilde{m} |z - \mathbf{x}|) K_0(\tilde{m} |\mathbf{y} - \mathbf{x}|) \right] \end{aligned} \quad (5)$$

for the unpolarized component and

$$\begin{aligned} \Phi_{pol} = \frac{2\alpha_s}{\pi} \tilde{m}^2 \alpha (1 - \alpha) \left[ \frac{z^2 - x^2}{|z - \mathbf{x}|} K_0(\tilde{m} |\mathbf{y} - \mathbf{x}|) K_1(\tilde{m} |z - \mathbf{x}|) \right. \\ \left. + \frac{y^2 - x^2}{|\mathbf{y} - \mathbf{x}|} K_1(\tilde{m} |\mathbf{y} - \mathbf{x}|) K_0(\tilde{m} |z - \mathbf{x}|) \right] \end{aligned} \quad (6)$$

for the polarization-dependent part. Here  $\tilde{m} = m(1 - \alpha)$  with  $m$  the quark mass.

To describe the interaction with the target in Fig. 3 we use the Wilson line formalism in the  $A^+ = 0$  light cone gauge of the projectile (see [3] for a detailed description of the formalism). (Our light cone 4-vector components are defined by

$x^\pm = t \pm z$ .) Defining the fundamental representation Wilson line

$$V_{\mathbf{x}} \equiv \mathcal{P} \exp \left[ \frac{ig}{2} \int_{-\infty}^{+\infty} dx^+ T^a A^{-a}(x^+, x^- = 0, \mathbf{x}) \right] \quad (7)$$

we can write the  $S$ -matrix operator for a fundamental-representation color dipole scattering on the target proton or nucleus by

$$\hat{D}_{\mathbf{x}\mathbf{y}} \equiv \frac{1}{N_c} \text{Tr} [V_{\mathbf{x}} V_{\mathbf{y}}^\dagger]. \quad (8)$$

Using this object we can write the interaction with the target  $\mathcal{I}^{(q)}$  as

$$\begin{aligned} \mathcal{I}^{(q)} = \left\langle \hat{D}_{\mathbf{z}\mathbf{y}} + \hat{D}_{\mathbf{u}\mathbf{w}} - \frac{N_c}{2C_F} \hat{D}_{\mathbf{z}\mathbf{x}} \hat{D}_{\mathbf{x}\mathbf{w}} + \frac{1}{2N_c C_F} \hat{D}_{\mathbf{z}\mathbf{w}} \right. \\ \left. - \frac{N_c}{2C_F} \hat{D}_{\mathbf{u}\mathbf{x}} \hat{D}_{\mathbf{x}\mathbf{y}} + \frac{1}{2N_c C_F} \hat{D}_{\mathbf{u}\mathbf{y}} \right\rangle, \end{aligned} \quad (9)$$

where the first two terms are given by the graphs in the first line of Fig. 3.

Our goal is to find whether the quark production cross section (2) contributes to the STSA defined in Eq. (1). Clearly STSA should be given by the part of the cross section odd under the  $\mathbf{k} \rightarrow -\mathbf{k}$  interchange. STSA is usually thought of as arising from the  $(\vec{S} \times \vec{p}) \cdot \vec{k}$  term in the cross section, where  $\vec{S}$  is the spin of the incoming projectile and  $\vec{p}$  is its momentum: such term is  $T$ -odd. Analyzing Eq. (2) we see that the  $\mathbf{k} \rightarrow -\mathbf{k}$  transformation can be thought of as the  $\mathbf{z} \leftrightarrow \mathbf{y}$  coordinate interchange. The  $T$ -odd STSA-generating part results from the part of the integrand in Eq. (2) which is odd under the  $\mathbf{z} \leftrightarrow \mathbf{y}$  interchange: since the integrand is a product of  $\Phi_\chi$  and  $\mathcal{I}^{(q)}$  the  $T$ -odd contribution may arise in either of these terms. Because our lowest-order  $\Phi_\chi$  is symmetric under  $\mathbf{z} \leftrightarrow \mathbf{y}$ , at this level of approximation the STSA can only arise in the interaction with the target  $\mathcal{I}^{(q)}$ . Therefore we need to decompose Eq. (9) into the  $\mathbf{z} \leftrightarrow \mathbf{y}$  symmetric and anti-symmetric parts, with the latter one giving rise to STSA when used in Eq. (2).

Before we proceed to anti-symmetrize  $\mathcal{I}^{(q)}$ , let us pause and point out that the decomposition into the light cone wave function squared and the interaction with the target is quite general and is valid up to corrections suppressed by powers of energy, which are usually neglected in the high energy QCD framework. The conclusion that the  $T$ -odd STSA-generating term may arise either in the wave function squared or in the interaction with the target is also quite general. An example of the wave function squared giving the STSA-generating contribution is the initial-state Sivers effect [8], though, as was illustrated in [7], and as is also seen in Fig. 2, the wave function squared also includes final state splittings and interactions. Below we will construct the first ever example of the  $T$ -odd STSA-generating term generated in the interaction with the target.

To anti-symmetrize  $\mathcal{I}^{(q)}$  under the  $\mathbf{z} \leftrightarrow \mathbf{y}$  interchange we first need to decompose each dipole  $S$ -matrix into the even and odd pieces under the exchange of its

6 Yuri V. Kovchegov, Matthew D. Sievert

transverse coordinates, which corresponds to the  $C$ -parity operation exchanging the quark and the anti-quark [11, 12]:

$$\hat{D}_{\mathbf{x}\mathbf{y}} \equiv \hat{S}_{\mathbf{x}\mathbf{y}} + i \hat{O}_{\mathbf{x}\mathbf{y}} \quad (10a)$$

$$\hat{S}_{\mathbf{x}\mathbf{y}} \equiv \frac{1}{2} (\hat{D}_{\mathbf{x}\mathbf{y}} + \hat{D}_{\mathbf{y}\mathbf{x}}) \quad (10b)$$

$$\hat{O}_{\mathbf{x}\mathbf{y}} \equiv \frac{1}{2i} (\hat{D}_{\mathbf{x}\mathbf{y}} - \hat{D}_{\mathbf{y}\mathbf{x}}) . \quad (10c)$$

The  $C$ - and  $T$ -even part  $\hat{S}_{\mathbf{x}\mathbf{y}}$  is the “standard” dipole amplitude giving the total unpolarized DIS cross section in DIS. Its expression in terms of Wilson lines allows to include Glauber-Mueller multiple rescatterings [13] along with the nonlinear small- $x$  BK/JIMWLK evolution in the leading- $\ln s$  approximation. The  $C$ - and  $T$ -odd *odderon* amplitude  $\hat{O}_{\mathbf{x}\mathbf{y}}$  [14, 15, 16] starts out with the triple gluon exchange at the lowest order [17], but then can also be enhanced by the multiple rescatterings and small- $x$  evolution [18, 11, 12, 19].

Using the decomposition (10) we can split  $\mathcal{I}^{(q)}$  into the  $T$ - and  $C$ -even  $\mathbf{z} \leftrightarrow \mathbf{y}$  symmetric part and the  $T$ - and  $C$ -odd  $\mathbf{z} \leftrightarrow \mathbf{y}$  anti-symmetric part:

$$\begin{aligned} \mathcal{I}_{sym}^{(q)} = & \left\langle \hat{S}_{\mathbf{z}\mathbf{y}} + \hat{S}_{\mathbf{u}\mathbf{w}} - \frac{N_c}{2C_F} \left( \hat{S}_{\mathbf{z}\mathbf{x}} \hat{S}_{\mathbf{x}\mathbf{w}} - \hat{O}_{\mathbf{z}\mathbf{x}} \hat{O}_{\mathbf{x}\mathbf{w}} \right) + \frac{1}{2N_c C_F} \hat{S}_{\mathbf{z}\mathbf{w}} \right. \\ & \left. - \frac{N_c}{2C_F} \left( \hat{S}_{\mathbf{u}\mathbf{x}} \hat{S}_{\mathbf{x}\mathbf{y}} - \hat{O}_{\mathbf{u}\mathbf{x}} \hat{O}_{\mathbf{x}\mathbf{y}} \right) + \frac{1}{2N_c C_F} \hat{S}_{\mathbf{u}\mathbf{y}} \right\rangle, \end{aligned} \quad (11a)$$

$$\begin{aligned} \mathcal{I}_{anti}^{(q)} = & i \left\langle \hat{O}_{\mathbf{z}\mathbf{y}} + \hat{O}_{\mathbf{u}\mathbf{w}} - \frac{N_c}{2C_F} \left( \hat{O}_{\mathbf{z}\mathbf{x}} \hat{S}_{\mathbf{x}\mathbf{w}} + \hat{S}_{\mathbf{z}\mathbf{x}} \hat{O}_{\mathbf{x}\mathbf{w}} \right) + \frac{1}{2N_c C_F} \hat{O}_{\mathbf{z}\mathbf{w}} \right. \\ & \left. - \frac{N_c}{2C_F} \left( \hat{O}_{\mathbf{u}\mathbf{x}} \hat{S}_{\mathbf{x}\mathbf{y}} + \hat{S}_{\mathbf{u}\mathbf{x}} \hat{O}_{\mathbf{x}\mathbf{y}} \right) + \frac{1}{2N_c C_F} \hat{O}_{\mathbf{u}\mathbf{y}} \right\rangle . \end{aligned} \quad (11b)$$

The spin-dependent and spin-averaged cross sections  $d(\Delta\sigma)$  and  $d\sigma_{unp}$  for quark production from (1) read

$$\begin{aligned} d(\Delta\sigma^{(q)}) = & \frac{C_F}{(2\pi)^3} \frac{\alpha}{1-\alpha} \int d^2x d^2y d^2z e^{-i\mathbf{k}\cdot(\mathbf{z}-\mathbf{y})} \\ & \times \Phi_{pol}(\mathbf{z}-\mathbf{x}, \mathbf{y}-\mathbf{x}, \alpha) \mathcal{I}_{anti}^{(q)}(\mathbf{x}, \mathbf{y}, \mathbf{z}) \end{aligned} \quad (12a)$$

$$\begin{aligned} d\sigma_{unp}^{(q)} = & \frac{C_F}{2(2\pi)^3} \frac{\alpha}{1-\alpha} \int d^2x d^2y d^2z e^{-i\mathbf{k}\cdot(\mathbf{z}-\mathbf{y})} \\ & \times \Phi_{unp}(\mathbf{z}-\mathbf{x}, \mathbf{y}-\mathbf{x}, \alpha) \mathcal{I}_{sym}^{(q)}(\mathbf{x}, \mathbf{y}, \mathbf{z}) , \end{aligned} \quad (12b)$$

where the wave functions squared are given by Eqs. (5), (6), and the interactions are given by Eqs. (11). Eqs. (12) are the main results of this work: when substituted into Eq. (1) they give the single-transverse spin asymmetry  $A_N$  generated in quark production by the  $C$ - and  $T$ -odd interactions with the target.

### 3. Properties of the Obtained STSA

The expressions in Eqs. (12) are hard to evaluate in general. To understand the main properties of the STSA contribution resulting from our mechanism, we used the am-

plitudes  $S_{xy}$  and  $O_{xy}$  evaluated in the Glauber-Mueller [13] multiple-rescattering approximation and determined the corresponding STSA in the large- $N_c$  limit after making several crude approximations described in [1]. The results are summarized below.

### 3.1. Transverse Momentum and Feynman- $x$ Dependence

First of all, in the large- $k_T$  limit the STSA due to our mechanism is (assuming that the unpolarized cross section  $d\sigma_{unp}$  is dominated by gluon production)

$$A_N^{(q)} \Big|_{k_T \gg Q_s} \propto \frac{k^2}{k_T^6} \propto \frac{1}{k_T^5} \quad (13)$$

which is a steeply-falling function of  $k_T$ . This indicates that in the standard factorization framework our STSA generating mechanism originates in some higher-twist operator.

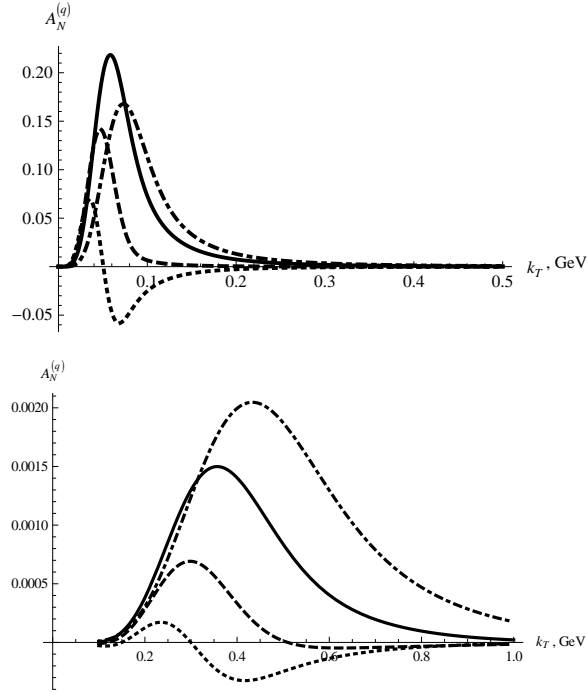


Fig. 4. Quark STSA in our mechanism for the proton target plotted as a function of  $k_T$  for different values of the longitudinal momentum fraction  $\alpha$  carried by the produced quark:  $\alpha = 0.9$  (dash-dotted curve),  $\alpha = 0.7$  (solid curve),  $\alpha = 0.6$  (dashed curve), and  $\alpha = 0.5$  (dotted curve). The infrared cutoffs are 2.1 fm in the top panel and 1.3 fm in the bottom panel.

The  $k_T$ -dependence of  $A_N$  is illustrated over a broader momentum range in Fig. 4. Note that the asymmetry is a non-monotonic function of  $k_T$  which even

8 *Yuri V. Kovchegov, Matthew D. Sievert*

changes sign (it has zeros/nodes). This seems to be in qualitative agreement with some of the experimental data on STSA. The maximum of  $A_N$  in the saturation framework is correlated with the saturation scale. Another important feature is that the asymmetry in Fig. 4 increases with the increasing momentum fraction  $\alpha$  (an analogue of the Feynman- $x$  variable) for most values of  $\alpha$ : this is also in qualitative agreement with experiment.

An important feature of our STSA is that it is proportional to

$$A_N^{(q)} \sim \int d^2b [\nabla T(\mathbf{b})]^2 \quad (14)$$

with  $T(\mathbf{b})$  the nuclear profile function. Since the variation of  $T(\mathbf{b})$  is largest in the peripheral collisions, our STSA seems to be dominated by large impact parameter scattering and is sensitive to the edges of the target. This explains the difference between the two panels in Fig. 4, which are different in the infrared cutoff used to limit the large- $b$  integration. A full analysis of the obtained formula without crude approximations made in [1] should determine whether the saturation scale is large enough in the peripheral collisions dominating STSA for the perturbative approach to be valid.

### 3.2. Atomic Number and Centrality Dependence

The dependence of our STSA on the size of the target for  $k_T \approx Q_s$  is

$$A_N^{(q)}(k_T \approx Q_s) \sim \frac{1}{Q_s^7} \sim A^{-7/6}, \quad (15)$$

if  $Q_s^2 \sim A^{1/3}$ . This is a very steep falloff of STSA with the atomic number of the nuclear target, which is also illustrated in Fig. 5, where  $A_N$  is plotted for several target radii. We thus predict that, in our formalism, STSA should be much smaller in the polarized proton–nucleus collisions than in the polarized proton–proton collisions.

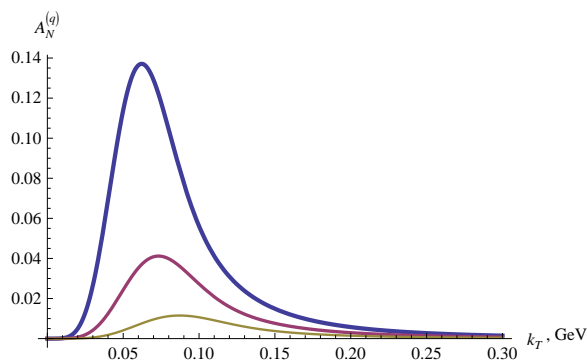


Fig. 5. Quark STSA in our mechanism plotted as a function of  $k_T$  for different values of the target radius:  $R = 1$  fm (top curve),  $R = 1.4$  fm (middle curve), and  $R = 2$  fm (bottom curve) for  $\alpha = 0.7$ .



### 3.3. STSA in Photon Production

The mechanism we employed allows one to calculate the STSA of prompt photons as well. The calculation yields [1]

$$d(\Delta\sigma^{(\gamma)}) = \frac{i}{(2\pi)^3} \int d^2x d^2y d^2z e^{-i\mathbf{k}\cdot(\mathbf{z}-\mathbf{y})} \Phi_{pol}(-\mathbf{z}, -\mathbf{y}, \alpha) \times [O_{\mathbf{x}+(1-\alpha)\mathbf{z}, \mathbf{x}+(1-\alpha)\mathbf{y}} - O_{\mathbf{x}, \mathbf{x}+(1-\alpha)\mathbf{y}} - O_{\mathbf{x}+(1-\alpha)\mathbf{z}, \mathbf{x}}] \quad (16)$$

where  $\Phi_{pol}$  is given by Eq. (5) with the  $\alpha_s \rightarrow \alpha_{EM} Z_f^2$  replacement. This expression is zero since

$$\int d^2x O_{\mathbf{z}+\mathbf{x}, \mathbf{y}+\mathbf{x}} = 0 \quad (17)$$

due to the fact that the odderon amplitude is an anti-symmetric function of its transverse coordinate arguments,

$$O_{\mathbf{x}\mathbf{y}} = -O_{\mathbf{y}\mathbf{x}}. \quad (18)$$

We thus have an exact result that in our mechanism the photon STSA is zero,

$$A_N^{(\gamma)} = 0, \quad (19)$$

at least in the order of approximation considered here.

### 4. Outlook

In the future it will be important to explore other ways of generating STSA in the saturation/CGC formalism. Above we studied STSA originating in the interaction with the unpolarized target. However, as we mentioned, it may also originate in the wave function squared. This would be the Siverts mechanism as studied in [7]. The analogue of this effect is illustrated in Fig. 6, where the STSA should be obtained by the interference between the diagrams in Figs. 6 and 2. The relative phase would

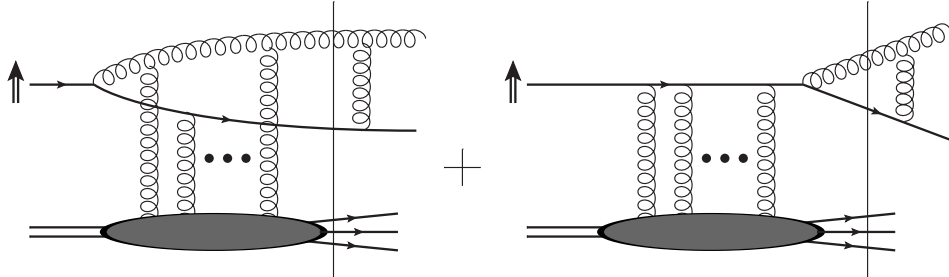


Fig. 6. Diagrams incorporating the Siverts effect into our formalism.

arise due to the extra rescattering with the polarized projectile, and is depicted by the cut giving the imaginary part. (Indeed Fig. 6 shows only one of the relevant diagrams.) The analysis of this contribution is left for future work [9].

10 Yuri V. Kovchegov, Matthew D. Sievert

## Acknowledgments

This research is sponsored in part by the U.S. Department of Energy under Grant No. de-sc0004286.

## References

1. Y. V. Kovchegov and M. D. Sievert, *A New Mechanism for Generating a Single Transverse Spin Asymmetry*, [arXiv:1201.5890](#).
2. E. Iancu and R. Venugopalan, *The color glass condensate and high energy scattering in QCD*, [hep-ph/0303204](#).
3. H. Weigert, *Evolution at small  $x_{bj}$ : The Color Glass Condensate*, *Prog. Part. Nucl. Phys.* **55** (2005) 461–565, [[hep-ph/0501087](#)].
4. J. Jalilian-Marian and Y. V. Kovchegov, *Saturation physics and deuteron gold collisions at RHIC*, *Prog. Part. Nucl. Phys.* **56** (2006) 104–231, [[hep-ph/0505052](#)].
5. Y. V. Kovchegov and A. H. Mueller, *Gluon production in current nucleus and nucleon nucleus collisions in a quasi-classical approximation*, *Nucl. Phys.* **B529** (1998) 451–479, [[hep-ph/9802440](#)].
6. J.-w. Qiu and G. F. Sterman, *Single transverse spin asymmetries in hadronic pion production*, *Phys.Rev.* **D59** (1998) 014004, [[hep-ph/9806356](#)].
7. S. J. Brodsky, D. S. Hwang, and I. Schmidt, *Final state interactions and single spin asymmetries in semi-inclusive deep inelastic scattering*, *Phys.Lett.* **B530** (2002) 99–107, [[hep-ph/0201296](#)].
8. D. W. Sivers, *Single Spin Production Asymmetries from the Hard Scattering of Point-Like Constituents*, *Phys.Rev.* **D41** (1990) 83.
9. Y. V. Kovchegov and M. D. Sievert, *Sivers effect in high energy QCD*, in preparation.
10. J. C. Collins, *Fragmentation of transversely polarized quarks probed in transverse momentum distributions*, *Nucl.Phys.* **B396** (1993) 161–182, [[hep-ph/9208213](#)].
11. Y. V. Kovchegov, L. Szymanowski, and S. Wallon, *Perturbative odderon in the dipole model*, *Phys.Lett.* **B586** (2004) 267–281, [[hep-ph/0309281](#)]. Dedicated to the memory of Jan Kwiecinski.
12. Y. Hatta, E. Iancu, K. Itakura, and L. McLerran, *Odderon in the color glass condensate*, *Nucl.Phys.* **A760** (2005) 172–207, [[hep-ph/0501171](#)].
13. A. H. Mueller, *Small  $x$  Behavior and Parton Saturation: A QCD Model*, *Nucl. Phys.* **B335** (1990) 115.
14. L. Lukaszuk and B. Nicolescu, *A Possible interpretation of  $p p$  rising total cross-sections*, *Lett.Nuovo Cim.* **8** (1973) 405–413.
15. B. Nicolescu, *The Odderon today*, *Presented at the Moriond 1990 Conference* (1990).
16. C. Ewerz, *The Odderon in quantum chromodynamics*, [hep-ph/0306137](#).
17. S. Jeon and R. Venugopalan, *A Classical Odderon in QCD at high energies*, *Phys.Rev.* **D71** (2005) 125003, [[hep-ph/0503219](#)].
18. J. Bartels, L. Lipatov, and G. Vacca, *A New odderon solution in perturbative QCD*, *Phys.Lett.* **B477** (2000) 178–186, [[hep-ph/9912423](#)].
19. A. Kovner and M. Lublinsky, *Odderon and seven Pomerons: QCD Reggeon field theory from JIMWLK evolution*, *JHEP* **0702** (2007) 058, [[hep-ph/0512316](#)].